Experimental and simulated cell migration in 1D and 2D nanofiber microenvironments

A THESIS SUBMITTED TO THE FACULTY OF THE UNIVERSITY OF MINNESOTA BY:

Horacio Michael Estabridis

IN PARTIAL FULFILLMENT OF THE REQUIREMENTS FOR THE DEGREE OF MASTER OF SCIENCE

David J. Odde

March, 2017

ACKNOWLEDGEMENTS:

I would like to express my deepest gratitude to my advisor David J. Odde. Without his help and support, both professional and personal, none of this work would have been possible. His passion and scientific insight have made me a better scientist and engineer. I am extremely thankful for the opportunity he gave me to conduct research under his guidance.

I would like to thank my labmates, especially Louis Prahl and Ghaidan Shamsan for their continuous help through my research. The ability to bounce ideas and learn new techniques was indispensable to the success of this project.

I would like to thank my mother and father, grandparents, aunts and uncles who fed my curiosity and sparked my interest in science, technology and medicine. Their love and support have put me on this path and pushed me to become a better professional and person. I cannot express my gratitude for their continued sacrifices.

I would like to thank my friends and mentors that have pushed me and supported me throughout the years. These relationships helped to mold me into a biomedical engineer and have given me the confidence to pursue this career path.

Financial support was provided by the University of Minnesota and the National Cancer Institute (Grant Number: R01 CA172986) .

I wish health, success and good fortune on all those who have helped me.

DEDICATION:

I would like to dedicate this work to my grandmother Pastora Natividad Estabridis, my parents Janet and Horacio Estabridis and my brother Andrew.

ABSTRACT:

Understanding how cells migrate in fibrous environments is important in wound healing, immune function, and cancer progression. A key question is how fiber orientation and network geometry influence cell movement. Here we describe a quantitative, modeling-based approach toward identifying the mechanisms by which glioblastoma cells migrate in fibrous geometries having well controlled orientation. Specifically, U251 glioblastoma cells were seeded onto STEP Fiber substrates that consist of networks of suspended 400 nm diameter nanofibers. Cells were classified based on the local fiber geometry and live cell migration was tracked, quantified and parameterized. Cells were found in three distinct geometries: adhering two a single fiber, adhering to two parallel fibers, and adhering to a network of orthogonal fibers. Cells adhering to a single fiber or two parallel fibers can only move in one dimension along the fiber axis, whereas cells on a network of orthogonal fibers can move in two dimensions. We found that cells move faster and more persistently in 1D geometries than in 2D, with cell migration being faster on parallel fibers than on single fibers. To explain these behaviors mechanistically, we simulated cell migration in the three different geometries using a motor-clutch based model for cell traction forces. Using nearly identical parameter sets for each of the three cases, we found that the simulated cells naturally replicated the reduced migration in 2D relative to 1D geometries. In addition, the modestly faster 1D migration on parallel fibers relative to single fibers was captured using a modest increase in the number of clutches to reflect increased surface area of adhesion on parallel fibers. Overall, the integrated modeling and experimental analysis indicates that cell migration response to varying fibrous geometries can be explained by a simple mechanical readout of geometry via a motor-clutch mechanism.

TABLE OF CONTENTS

LIST OF TABLES

LIST OF FIGURES

INTRODUCTION

Glioblastoma is an aggressive form of cancer that can quickly spread throughout a patient's brain using microstructural pathways, such as axon tracts and blood vessels (Cha, Kang, and Kim 2016). Understanding these avenues for the migration of glioblastoma cells through the brain, and cell migration along oriented structural features generally, represents an aspect of the disease that could potentially be targeted by new treatment options. Development of an *in vitro* system, and a computational model that explains behavior in it, could elucidate migration mechanisms and aid more generally in the development of potential treatment strategies for processes that rely on cell migration along defined structural features.

Toward this goal, we explored the use of STEP Fibers as a nanoscale system that somewhat replicates the architecture of the routes of invasion in glioblastoma along capillary and axonal structures. STEP Fiber arrays contain within them diverse, complex geometries with ability to control fiber material type, diameter, orientation, and spacing (Nain and Wang 2013). The fabrication process generates two regions of crossed nanowires having diameters of approximately 400 nm in a net-like pattern with regions of freely spanning nanofibers in between (Nain and Wang 2013) (Figure 1A). Cells that adhere to the net-like regions of the STEP Fiber substrate locally experience two-dimensional (2D) orthogonal fiber geometries, whereas cells in the free span regions of the substrates are restricted to one-dimensional (1D) environments composed of parallel fibers (Figure 1A). In the 1D regions, cells encounter two distinct geometries, one where cells adhere to two parallel fibers with the cell body "straddling" the space between the two spans, and another where they adhere to only one individual fiber. Additionally, STEP Fiber substrates are mechanically anisotropic: though made of crystalline polystyrene (Elastic Modulus = 3.5 GPa) the diameter of the nanofibers is such that cells

have the ability to deflect the free span regions when applying a mechanical load laterally. However, cells are not predicted to be able to generate sufficient force to buckle a nanofiber through axial loading, and such buckling is not observed experimentally. Since brain tissue is neither homogeneous nor isotropic, it would be useful to have inhomogeneous and anisotropic microenvironments that replicate these features *in vitro*. The combination of a variety of defined geometries and mechanical anisotropy makes the STEP Fiber substrate a unique experimental system that has useful properties distinct from other microfabricated systems used to study cellular migration, such as micro-patterned lanes (Sniadecki et al. 2006), channels (Faure-andré et al. 2008), and 2D surfaces (Lämmermann and Sixt 2009).

Using the DBTRG-05MG glioblastoma cell line the Nain research group studied blebbing dynamics of cells on STEP Fiber substrates (Sharma et al. 2013). They found that cells exhibit three primary morphologies while adhering to these substrates: spindle, rectangular and polygonal (Sharma et al. 2013). The spindle morphology was associated with cells that were suspended on one single fiber while, the rectangular morphology was associated with cells that were adherent to two parallel fibers. Finally, the polygonal morphology was associated with cells that were adherent to orthogonal fibers or were in the net region of the fiber substrate. The geometry-driven morphology affected the blebbing dynamics of the DBTRG-05MG cells, and appeared to affect the speed at which the cells migrated (Sharma et al. 2013). It is these geometry-driven differences that have motivated the present study of U251 cells on these substrates and informed the hypothesis that these fibers could be applied to replicate brain architecture. While the study by Sharma *et al.* established that geometry affected cellular behavior, it did not explain the mechanisms that drove these differences, which we now address.

In order to develop a mechanistic understanding, a stochastic model of cellular migration was developed based on our published 2D cell migration simulator (Klank

2016, in press). The cell migration simulator models the action of individual adhesion proteins (termed “clutches”) and myosin motor proteins (termed “motors”) (Chan and Odde 2008; Klank 2016, in press). The speed of a simulated cell is very sensitive to the ratio of motors to clutches (Bangasser, Rosenfeld, and Odde 2013). Previous studies using this simulator revealed that cell adhesivity controls the speed of glioma cell migration and correlates with CD44-mediated migration of mouse glioblastoma cells in intact brain slices (Klank 2016, in press). High and low concentrations of CD44 will lead to lower cell speed. However, intermediate CD44 concentrations significantly increase cell speed (Klank 2016, in press). Importantly, this study revealed that cell migration speed is anti-correlated with mouse and human disease survival. Intermediate adhesivity values lead to the fastest migration in mice and the worst survival outcomes in mice and humans (Klank 2016, in press). To use this cell migration simulator to predict cmigration behavior in fibrous environments, we need to incorporate the mechanical features of the nanofibers, such as their stiffness, mechanical anisotropy, orientation, diameter, and spacing. Adding the environmental inhomogeneity and mechanical anisotropy to this model therefore allowed us to investigate the mechanisms that modulate cellular behavior on these STEP fibers.

RESULTS

Persistent random walk and random walk models can be used to parameterize cellular migratory behavior in 1D and 2D, respectively

To investigate the migratory behavior of GFP-actin U251 cells on STEP fibers, cells were imaged via phase contrast and fluorescence microscopy for five hours at 15 minute intervals. The three different geometries observed were: cells on single fibers ($n = 90$), cells spanning two parallel fibers ($n = 94$) and cells on net structures ($n = 97$) (Figure 1A - E). Cell centroids were then tracked as cells migrated on the fibrous structures (Figure 2A - C). The cells were categorized based on the local geometry of the STEP nanofiber (Sharma et al. 2013). During the experiment nanofibers were oriented at random angles in the field of view. As a result, coordinate systems for each cell were rotated to ensure that the nanofibers were oriented along a major axis. The single and parallel fiber geometries that were restricted to 1D motion had their coordinate systems rotated clockwise such that the nanofiber was parallel to the x-axis. The net fibers had their coordinate systems rotated clockwise to ensure that the fibers and their orthogonal partners aligned with either the x-axis or y-axis. Cellular migration can be modeled as a stochastic process, at its simplest either as a random walk or a persistent random walk (Wirtz 2009). Mean squared displacement (MSD) time series were calculated for each cell in the three geometric conditions from the position data generated by particle tracking. The MSD data was used to characterize and quantify the migration behavior of cells in the three different geometries. Because cells can exhibit persistent behavior when traveling in 1D or oriented environments (Fraley et al. 2012) (Curtis and Wilkinson 1997) we tested weather a persistent random walk model was appropriate for describing cell trajectories. The same cells do not appear to exhibit this

behavior when traveling on the 2D net structures and trajectories more closely resembled a random walk. Since our imaging frequency was 15 min any persistence values that fell below the 15 min threshold could not be confidently measured by our experiment. In this case the migration model would collapse to a simple random walk.

$$MSD(t) = nS^2P^2(e^{\frac{-t}{P}} + \frac{t}{P} - 1)$$ **[1]** (Wu et al. 2014)

$$MSD(t) = 2nDt$$ **[2]** (Wu et al. 2014)

Equation 1 is the persistent random walk model where n is the number of dimensions in which motion is occurring ($n = 1$ for single and parallel fibers, $n = 2$ for net structures), t is the time, S is the speed of the cell and P is the persistence time. A special case of the persistent random walk is the random walk model, given by Equation 2 when $P = 0$, where D is the random motility coefficient. It is qualitatively clear from the MSD-versus-time data that cells in the three different geometries exhibit distinct behaviors (Figure 2D). MSD values for 1D motion (single and parallel fibers) are an order of magnitude higher than the net fibers (Figure 2D). This is despite the fact that cells moving in 1D have one less degree of freedom than cells moving in 2D. To parameterize and quantify cell behavior on the three different geometries the MSD-versus-time data was fit to both of these models (Figure 3A - C). We determined that the two parameter persistent random walk model is a more appropriate approximation of single and parallel fiber MSD-versus-time data sets via the Bayesian Information Criterion (BIC). When fitting with a persistent random walk model to the single and parallel fiber geometries an ≈20% reduction in BIC was observed for the persistent random walk model as opposed to the random walk model (single fiber ΔBIC = 21%, parallel fiber ΔBIC = 24%). The net fiber geometry did not have a significant improvement for the persistent random walk BIC value over the random walk (ΔBIC = -2%). Additionally, the persistence value extracted from the model fit was two orders of

magnitude smaller than our 15 min sampling time ($P_{Net} = 0.4\,min$). Therefore a random walk model is more appropriate to describe the 2D motion of the net structures (Figure 3C). Each model was fit to the average MSD-versus-time data (Figure 3A - B). The distribution of parameter values was estimated from the 95% parameter confidence intervals. The increase in cell persistence and MSD magnitude between 1D and 2D motion occurs despite the fewer degrees of freedom cells have when moving on 1D substrates.

Cells have a longer persistence time when adhering to two parallel fibers

The persistence of cells was assessed in two ways: first, the estimated distribution of persistence parameters extracted from the persistent random walk fits were analyzed for a statistically significant shift via Student's t-test. It was found that the average persistence time of 165 min for the parallel fiber cells was significantly higher than the 61 min average value for the single fiber cells ($\mathrm{p} << 0.01$) (Figure 4C). The second method which was used to analyze the persistent behavior of cells in 1D geometries was autocorrelation analysis of the displacements of each cell between each sample time point (Odde et al. 1996). Displacements were calculated for each cell in both the single fiber ($\mathrm{n} = 90$) and parallel fiber geometries ($\mathrm{n} = 94$). The vector of displacements for each cell was autocorrelated and an exponential decay function was fitted to it (Figure 4A). The decay time extracted from the autocorrelation fit represents a persistence time that gives the average amount of time a cell spent traveling in a direction before reversal. It was found that the average of persistence times for parallel fibers ($\mu = 31\ \mathrm{mins}$) was again higher than that of the single fibers ($\mu = 21\ \mathrm{mins}$) via Dunn-Sidak post-hoc statistical analysis ($\alpha = 0.05$) (Figure 3B).

Stochastic cell migration model captures cellular behavior on STEP fibers

In order to better understand the mechanistic basis of the faster migration in 1D vs. 2D, and the higher persistence on parallel fibers vs. single fibers, a stochastic cell simulator was developed to replicate the mechanical environment of the STEP Fiber substrate. Cell migration was simulated using the cell migration model as previously described (Klank et al., in press), except with modification to allow for spatial inhomogeneity and mechanical anisotropy in the cellular environment, as described in the methods section. Approximately ninety simulations were run on each geometry to generate a simulated dataset similar in size to the experiments (Single Fibers = 90, Parallel Fibers = 91 and Net Fibers = 91). The simulations were then analyzed using the same procedures as the experiments. The simulated cells were able to match the MSD of the different experimental geometries (Figure 5C - D & F). The simulations also matched the distribution of persistence times extracted from the persistent random walk fit applied to the experimental MSD-versus-time data of the single ($\mu_{experiment} = 61\ min, \mu_{simulation} = 62\ min$) and parallel fiber geometries ($\mu_{experiment} = 165\ min, \mu_{simulation} = 192\ min$). There was a wider distribution of simulated persistence values (Single Fibers: $\sigma_{experiment} = 24\ min, \sigma_{simulation} = 35\ min$, Parallel Fibers: $\sigma_{experiment} = 56\ min,\ \sigma_{simulation} = 95\ min$) as opposed to the experimental persistence times. The distribution of simulated random motility coefficients is within the same order of magnitude as the experimental distribution ($\mu_{experiment} = 0.6104\ {\mu m^2}/{min}$, $\mu_{simulation} = 0.5414\ {\mu m^2}/{min}$). The simulated single fiber and parallel fiber cells however did not have a statistically significant difference in persistence as measured by the displacement autocorrelation analysis.

Amongst the simulated geometries, the only parameters that varied between simulated cells were the motor-clutch ratios. In order to match the experimental behavior the motor-clutch ratios were modified in each geometry. Only the number of clutches was changed in order to increase or decrease the ratio. The single fiber geometry had a motor-clutch ratio of 0.926, the parallel fiber geometry had a motor-clutch ratio of 0.735, and the net fiber geometry had a motor-clutch ratio of 1. The difference in motor-clutch ratios in these different geometries leads us to conclude that changes in adhesion is able to explain of the differences in cellular behavior in these different geometric conditions. The doubling of potential adhesive surface area for cells spanning two parallel fibers increases the persistence of these cells as the increased number of adhesions reduces the chances of reversing direction. The decrease in the motor-clutch ratio shows that increased adhesion in 1D migration can increase the persistence of this migration. This may explain why cells in channels tend to move persistently (Faure-andré et al. 2008). However, increase in adhesive surface area will eventually hinder cellular migration. A motor-clutch ratio >1 was found to significantly hinder simulated migration on the two dimensional net fiber geometry. This further explains the biphasic nature of cellular migration that has been previously described in studies of substrate stiffness (Chan and Odde 2008; Elosegui-Artola et al. 2016; Bangasser, Rosenfeld, and Odde 2013).

DISCUSSION

In this study we investigated the cellular response to varying geometries through a combination of experimental parameterization and theoretical simulation. Our experimental analysis shows that cells traveling on parallel fibers exhibit increased persistence, as compared to cells traveling on single fibers or two dimensional nets. Our experiments further reinforce the evidence that cells move faster when they are migrating under geometric constraints. Our simulations revealed that an increase in adhesivity in a 1D environment is a potential explanation for this increase in persistence on parallel fibers relative to single fibers. Using a simple model of the experimental mechanical and geometric environment we simulated and recreated the behavior of the three different geometries *in silico*. These results give us quantitative evidence that the speed and persistence of phenomena such as contact guidance (Provenzano et al. 2008) and glioblastoma migration in human brain tissues (Cha, Kang, and Kim 2016; Baker et al. 2014; Ivkovic et al. 2012) can be explained simply by both geometry and adhesivity, and does not necessarily require phenotypic or molecular expression changes.

Limitations of study

While STEP Fibers provide a great number of experimental advantages such as the ability to study cellular migration in a complex yet well characterized mechanical structure it does carry some disadvantages. The quality of our images was significantly reduced due to the suspended nature of the STEP fibers. The fibers are suspended approximately 0.8 mm above the glass of the 35 mm MatTek No. 0 glass bottom dishes (MatTek Corporation, Ashland, MA) used for the experiments. This distance is longer than the working distance of higher numerical aperture objectives on an inverted

microscope that require water or oil immersion and provide greater image quality. One solution would be to use an upright microscope and submerge the object lens in the media above the STEP fibers during experimental observation. This constraint on the type of microscope to generate higher resolution images is a limitation of the substrate. Additionally, our experiments had relatively low sampling frequency with one image taken every fifteen minutes. This allowed us to observe more cells in one experiment at the cost of reducing the temporal resolution of cellular migration. Our experiments do not provide a rigorous quantitative analysis of cell migration on short time scales (<15 min).

Our simulations, while able to provide good agreement with the experimental data, were limited by their two dimensional nature. Experimental cells in the parallel fiber geometry were shown to have a statistically significant increase in persistence through the displacement autocorrelation analysis. There are features that we could not account for in our simulations such as the three-dimensional spatial distribution of adhesion molecules that could stabilize the cell and reduce the probability of changing directions. Our stochastic model works by concentrating all adhesions in a cellular protrusion to one point in space. There is also a probability built into our simulations that will randomly disengage a protrusion, significantly reducing the stability of simulated cellular protrusions as opposed to the experiment. This lack of simulated protrusion stability and adhesion distribution likely is the reason the displacement autocorrelation analysis did not show a significant difference in the simulated cells.

STEP fibers as a potential *in vivo* mimic of tissue microstructures

The STEP fiber substrate has a significant number of mechanical properties that popular 3D culture methods do not have. Culturing cells *in vitro* in collagen, fibrin or Matrigel (Corning Inc., Tewksbury, MA), while significantly more physiologically relevant than 2D culture methods, has difficulty approaching mechanical stiffnesses comparable

to *in vivo* tissues. For example, collagen gels can have elastic modulus values of around 700 Pa (Yang, Leone, and Kaufman 2009). However, axons and *in vivo* extra cellular matrix (ECM) have been measured to have elastic modulus values of 12,000 Pa and 4000 Pa respectively (Javid, Rezaei, and Karami 2014). The elastic moduli of EMC is highly heterogeneous spatially and extremely anisotropic. The STEP fibers provide a way to achieve a mechanically well-characterized engineered structure that has the mechanical anisotropy of *in vivo* structures combined with orders of magnitude higher stiffness values. Further development of this technology could potentially yield more accurate *in vitro* tissue mimics that can recapitulate important aspects of the *in vivo* complexity of both geometric and mechanical environments.

Theoretical framework for prediction of migratory behavior

This research outlines a predictive model-driven approach that can be applied to cellular migration in different geometries and mechanical environments. Our ability to simulate and replicate the migratory behavior of cells *in vitro* can be used to test predictions of cellular behavior in new mechanical or geometric contexts. Experiments utilizing our parameter set and STEP fibers coated with different matrix constituents that cells commonly adhere to could elucidate the matrix constituents on which glioma cells migrate most effectively and explore the heterogeneity both within and between tumors of the same cancer subtype. There are many opportunities for the application of these methods to uncover new behaviors and mechanisms and further study is warranted to probe these questions.

MATERIALS AND METHODS

STEP Fiber cell culture

Glioblastoma U251 cells stably expressing GFP-Actin (Marsick, San Miguel-Ruiz, and Letourneau 2012) were cultured in Gibco® Opti-MEM® media (Invitrogen Corporation, Carlsbad, CA, USA) containing 10% fetal bovine serum. $400\ \mathrm{nm}$ diameter polystyrene STEP Fiber substrates (Nain and Wang 2013) were tacked down using Dow-Corning® High Vacuum Grease (Dow-Corning Inc., Midland, MI, USA) onto MatTek No. 0 glass bottom 35mm dishes (MatTek Corp., Ashland, MA, USA). The STEP Fiber substrate was incubated with $1\ mg/ml$ bovine plasma fibronectin (Sigma-Aldrich Inc., St. Louis, MO, USA) for four hours prior to cell seeding. Fifty microliters of cell suspension was seeded onto fibronectin-coated STEP fiber substrates at a concentration of $100{,}000\ {}^{cells}/_{mL}$ and incubated for three hours prior to imaging.

Cell migration imaging

Cells were imaged with a Nikon Instruments Eclipse Ti-E (Nikon Instruments Inc., Melville, NY, USA) for five hours at fifteen minute intervals. Images were captured with a Andor Zyla 5.5 sCMOS camera (Andor Technology Ltd., Belfast, Northern Ireland, UK). Widefield phase contrast images were collected with a Nikon 20x air phase ring objective lens (Nikon Instruments Inc., Melville, NY, USA) and GFP channel images were collected with illumination from a Cool LED pE-100 LED fluorescent illumination bank (CoolLED Ltd., Andover, England, UK). Cells were kept alive on the microscope through the use of AirTherm ATX (World Precision Instruments Inc., Sarasota, FL, USA). Time-lapse image collection was driven by NIS-Elements software (Nikon Instruments Inc., Melville, NY, USA).

Image processing and data analysis

Cells were classified based on which geometry the cell spent the majority of its time in the time-lapse movie. Wide-field GFP image stacks were cropped to select individual cells and thresholded using ImageJ (National Institutes of Health (NIH), Bethesda, MD, USA). Thresholded image stacks were fed into MATLAB and cell centroids were tracked using software developed in MATLAB 2012a and 2016a (MathWorks Inc., Natick, MA, USA) as previously described (Klank 2016, in press). The cell tracking software works by applying a binary filter to the grayscale images. Using MATLAB's image processing tool box, objects are labeled and the cell the user wishes to track is manually selected. Cell centroid positions are calculated for each frame for the object the user selects. Cell position data is saved to a plaintext file that can be read back into MATLAB for further processing. Coordinate systems were rotated using MATLAB, which used angles that were calculated in ImageJ. Mean Squared Displacement was calculated in MATLAB. Random walk and persistent random walk fits were conducted using MATLAB Curve Fitting Toolbox. Statistical tests were conducted using the MATLAB Statistics Toolbox.

Stochastic Cell Migration Simulator Description

The cell migration simulator works by simulating the action of individual adhesion molecules (termed "clutches"), myosin motor proteins (termed "motors"), and actin subunits, which self-assemble at the leading edge to form simulated cellular protrusions that displace the centroid of simulated cell, as previously described (Klank et al., in press). Briefly, the total starting amount of each of these three molecular species is fixed, ensuring mass conservation of key species. Upon initialization, cell protrusions extend at randomly chosen angles with a fixed initial length. Each time a new cellular protrusion is nucleated it removes the actin required to form it from the pool of F-actin

the cell has initially. Each protrusion is populated with a random number of clutches and motors which is subtracted from the total amount in their respective starting pools. The clutches are able to interact stochastically with the substrate to allow clutch binding and unbinding. Simultaneously, the F-actin in the protrusion is pulled back by the motors, at a velocity given by a linear force-velocity relationship, thus creating a displacement which simulates actin retrograde flow (He et al. 2015). In order to simulate the well-documented phenomenon of cellular sensitivity to substrate stiffness (Discher, Janmey, and Wang 2005) the substrate and the clutch is modeled as a linear spring. The clutch springs are arranged in parallel and connected in series with the substrate spring. The displacement generated by the actin retrograde flow generates reaction forces on the clutch and substrate springs. This series of events is happening simultaneously in every protrusion in the cell. Once force is generated, an elastic force balance equation is solved. This force balance, combined with the random orientation of force-generating protrusions, leads to cellular displacement. The forces generated can also cause protrusions to detach from the substrate: the more force that a clutch experiences, the higher the unbinding probability according to Bell's Law given by the following equation:

$$k_{off} = k_{off,0} \cdot e^{\frac{F}{F_B}} \quad \textbf{[3]}$$

This sudden protrusion failure will also have the effect of displacing the cell as the forces must rebalance with fewer protrusions. When retrograde flow causes the clutches to pass beyond the myosin motors the protrusion disassembles and the actin, motors and clutches are added back to their respective original pools. Thus performing a mass balance in the simulated system. A new protrusion may then be born with these components again restarting the process. This model of cellular migration has been well-characterized and it has been found that the two most sensitive parameters are the total number of motors and clutches (Bangasser, Rosenfeld, and Odde 2013).

Each geometry was modeled by restricting the region that cells can adhere to the surface. The single fiber geometry was modeled as a 400π nm wide lane with a uniform stiffness ($220\ {}^{pN}/_{nm,}$). The parallel fiber geometry was modeled as two parallel 400π nm wide lanes separated by 4000 nm. The parallel fiber geometry's mechanical anisotropy was modeled using a model based on Euler-Bernoulli beam theory:

$$\kappa_{sub} = \left| \frac{\pi E r^2}{L} \cdot \cos(\theta) + \frac{12\pi E r^4}{L^3} \cdot \sin(\theta) \right| \textbf{ [4]}$$

The first coefficient in the equation $\frac{\pi E r^2}{L}$ represents the spring constant experienced when the cell is loading the fiber laterally ($\theta = 0^0$). The second coefficient $\frac{12\pi E r^4}{L^3}$ represents the cell is loading the fiber orthogonally ($\theta = 90^0$). The net fiber geometry was modeled as a series of orthogonal lanes of uniform stiffness ($220\ {}^{pN}/_{nm,}$). The gap width between each fiber was identical to the parallel fiber geometry (4000 nm).

TABLES AND FIGURES

TALBE LEGENDS

Table 1: *Simulation Parameter Values*. Table contains a breakdown of the parameter values used in stochastic cell migration simulations for each geometry. Sources, justification and derivation of each parameter is outlined.

FIGURE LEGENDS

Figure 1: *Experimental Setup and Description of the Three Geometries Encountered By U251 Cells.* **(A)** A schematic cartoon diagram of the STEP fiber substrate. Cells in the three different geometric environments are labeled **C**, **D** and **E**. **(B)** GFP (top) and phase contrast (bottom) image of U251 GFP-Actin expressing cells seeded onto STEP Fiber substrates. Cells were imaged for five hours at fifteen minute intervals. Red boxes identify the three different geometries that cells encounter **C**,**D** and **E**. **(C)** GFP (L) and phase contrast (R) image of a cell on a single fiber (region "**C**" from **Fig. 1B**). **(D)** GFP (L) and phase contrast (R) image of a cell straddling two parallel fibers (region "**D**" from **Fig. 1B**). **(E)** GFP (L) and phase contrast (R) image of a cell suspended on a fiber network (region "**E**" from **Fig. 1B**).

Figure 2: *Position vs. Time Plots and Average Mean Squared Displacement for Each Experimental Geometry*. **(A)** GFP channel video (Supplement) (L) and 1D Position-versus-time plot (R) for a cell on a single fiber. **(B)** GFP channel video (Supplement) (L) and 1D Position-versus-time plot (R) for a cell on two parallel fibers. **(C)** GFP Channel video (300 min) (Supplement) (L) and a 2D position plot (R) for a cell on net fiber structure. **D)** Average Mean Squared Displacement for all cells in each geometry.

Figure 3: *Comparison of Persistent Random Walk and Random Walk Models to Experimental Average Mean Squared Displacement.* **(A)** Comparison of the two models fitting the experimental average mean squared displacement data of the single fiber geometry. (Random Walk BIC = 232.9 > Persistent Random Walk BIC = 184.3) **(B)** Comparison of the two models fitting the experimental average mean squared displacement data of the parallel fiber geometry. (Random Walk BIC = 260.6 > Persistent Random Walk BIC = 197.2). **(C)** Random Walk model fit to average mean squared displacement of net fiber geometry (Random Walk BIC = 138.3 < Persistent Random Walk BIC = 141.2).

Figure 4: *Increased Persistence for Cell Migrating in the Parallel Fiber Geometry.* **(A)** Average displacement autocorrelation for cells in single fiber and parallel fiber geometry. Displacement autocorrelation is calculated by finding the displacement between each time point for each cell and performing an autocorrelation (Odde et al. 1996). **(B)** Cells that are seeded onto single fibers or parallel fibers display persistent motion. Cells traveling on two parallel fibers have a longer persistence time than cells that are only on one single fiber. This difference in persistence time is statistically significant ($\alpha = 0.05$) showing that persistent motion is stronger when cells are adherent to two fibers. **(C)** Using parameters extracted from persistent random walk fitting of average behavior of cells we observe that there is a significant difference in persistence times between the single and parallel fiber geometries. Persistence was found to be $\mu = 61\ mins$ for single fibers geometry and $\mu = 165\ mins$ for parallel fibers geometry.

Figure 5: *Simulation of Cellular Migration in a 2D Stochastic Model of Each Geometry Replicates Experimental Behavior.* **(A)** Trajectory of single fiber simulation **(B)** Trajectory of parallel fiber simulation **(C)** Comparison of average experimental and simulated MSD for the single fiber geometry. **(D)** Comparison of average experimental

and simulated MSD for the parallel fiber geometry. **(E)** Trajectory of net fiber simulation (300 min simulation) **(F)** Comparison of average simulated and experimental MSD for net fiber geometry with average random walk fits to simulation ($\mathrm{Avg.\,RMC} = 0.6104\ {\mu m^2}/{min}$) and experiment ($\mathrm{Avg.\,RMC} = 0.5414\ {\mu m^2}/{min}$).

TABLE 1

Symbol	Parameter	Single Fiber Value	Parallel Fiber Value	Net Fiber Value	Source
N_m	Total number of motors	125	125	125	Adjustable (estimated based on (Molloy et al. 1995))
N_c	Total number of clutches	135	170	125	Adjustable (N_m/N_c based on (Bangasser, Rosenfeld, and Odde 2013))
A_{tot}	Total possible actin protrusion length	100 μm	100 μm	100 μm	Typical cell length
v_p*	Maximum actin polymerization velocity	200 nm/s	200 nm/s	200 nm/s	(Chan and Odde 2008)
k_{mod}*	Maximum module birth rate	1 s^{-1}	1 s^{-1}	1 s^{-1}	(Klank 2016, in press)
k_{mod}	Typical module birth rate	0.00001 s^{-1}	0.00001 s^{-1}	0.00001 s^{-1}	Must be similar to k_{cap}
k_{cap}	Module capping rate	0.00001 s^{-1}	0.00001 s^{-1}	0.00001 s^{-1}	Lowered from (Klank 2016, in press) to match experiments
l_{init}	Initial module length	1.5 μm	1.5 μm	1.5 μm	Adjustable
l_{min}	Minimum module length	0.1 μm	0.1 μm	0.1 μm	Adjustable
κ_{cell}	Cell spring constant	1000 pN/nm	1000 pN/nm	1000 pN/nm	Adjustable
$n_{c,cell}$	Number of cell body clutches	1	1	1	Adjustable ($<N_c$)
n_m*	Maximum number of module motors	25	25	25	Adjustable ($0.2*N_m$)
F_m	Motor stall force	2 pN	2 pN	2 pN	(Molloy et al. 1995)
v_m*	Motor unloaded velocity	120 nm/s	120 nm/s	120 nm/s	(Chan and Odde 2008)
n_c*	Maximum number of module clutches	27	34	25	Adjustable ($0.2*N_c$)
k_{on}	Clutch on-rate	1 s^{-1}	1 s^{-1}	1 s^{-1}	Increased from (Chan and Odde 2008)
k_{off}*	Clutch unloaded off-rate	0.1 s^{-1}	0.1 s^{-1}	0.1 s^{-1}	(Lele et al. 2008)
κ_c	Clutch spring constant	0.8 pN/nm	0.8 pN/nm	0.8 pN/nm	(Bangasser, Rosenfeld, and Odde 2013)
F_b	Clutch bond rupture force	2 pN	2 pN	2 pN	(Jiang et al. 2003)
κ_{sub}	Substrate spring constant	220 pN/nm	220 – 1 pN/nm	220 pN/nm	Estimated from Euler-Bernoulli beam theory, Equation 3

FIGURE 1

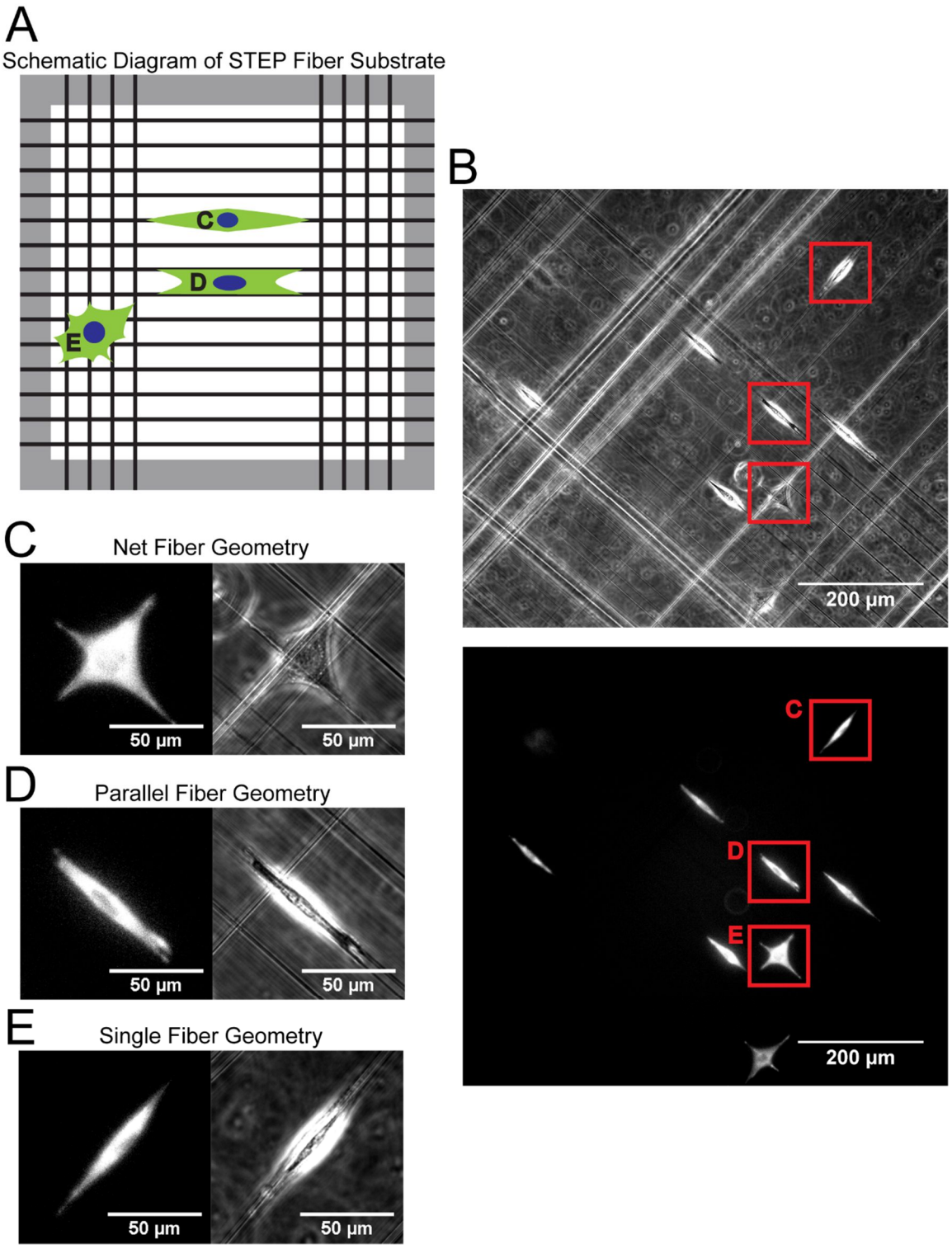
A
Schematic Diagram of STEP Fiber Substrate
C
D
E
B
200 µm
C
D
E
200 µm
C
Net Fiber Geometry
50 µm
50 µm
D
Parallel Fiber Geometry
50 µm
50 µm
E
Single Fiber Geometry
50 µm
50 µm

FIGURE 2

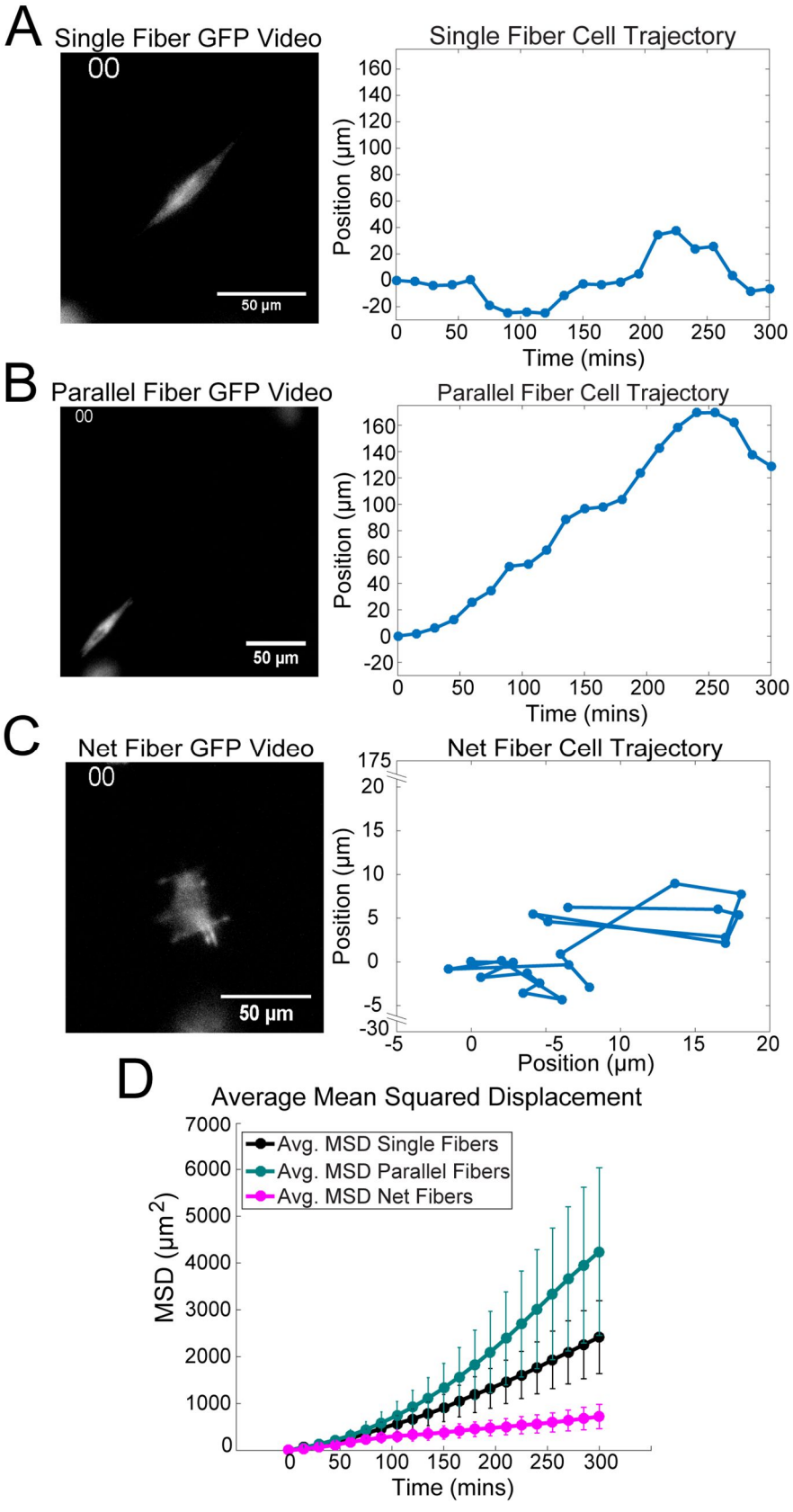
A
Single Fiber GFP Video
00
50 µm
Single Fiber Cell Trajectory
Position (µm)
Time (mins)
B
Parallel Fiber GFP Video
00
50 µm
Parallel Fiber Cell Trajectory
Position (µm)
Time (mins)
C
Net Fiber GFP Video
00
50 µm
Net Fiber Cell Trajectory
Position (µm)
Position (µm)
D
Average Mean Squared Displacement
Avg. MSD Single Fibers
Avg. MSD Parallel Fibers
Avg. MSD Net Fibers
MSD (µm2)
Time (mins)

FIGURE 3

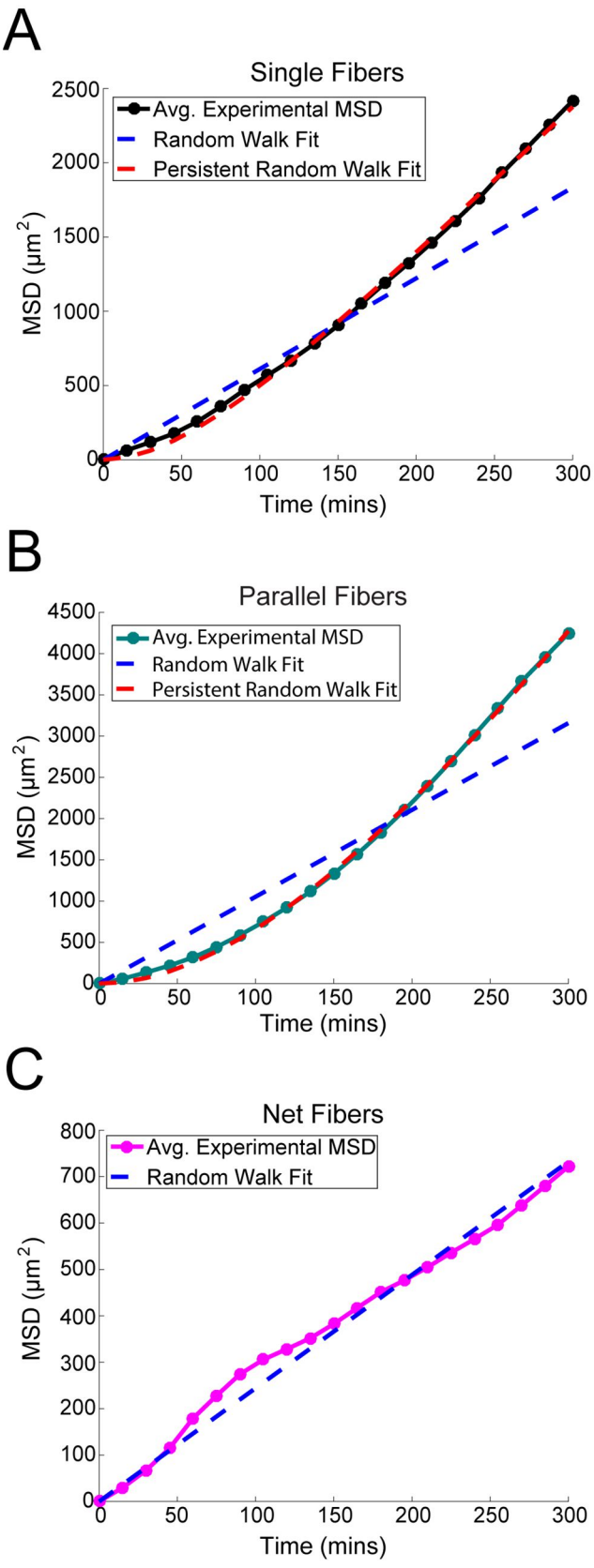
A
Single Fibers
Avg. Experimental MSD
Random Walk Fit
Persistent Random Walk Fit
MSD (μm²)
Time (mins)
B
Parallel Fibers
Avg. Experimental MSD
Random Walk Fit
Persistent Random Walk Fit
MSD (μm²)
Time (mins)
C
Net Fibers
Avg. Experimental MSD
Random Walk Fit
MSD (μm²)
Time (mins)

FIGURE 4

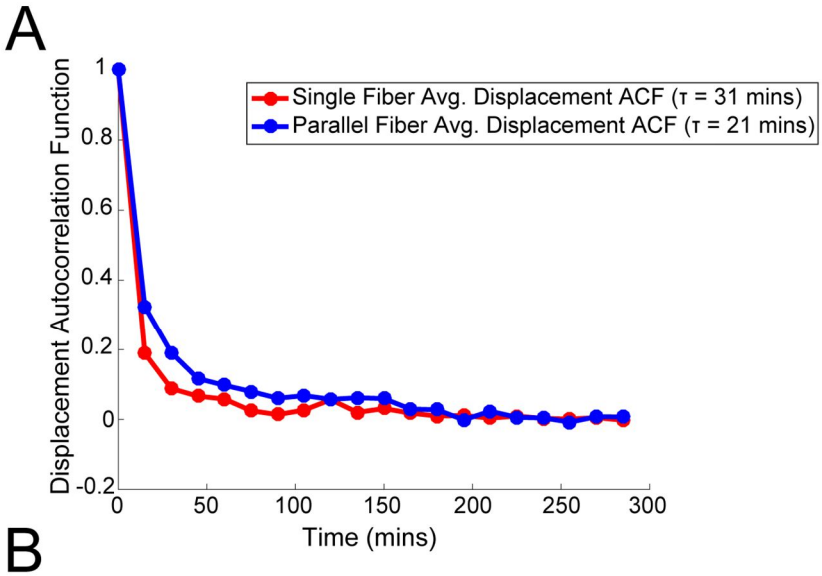
A
Single Fiber Avg. Displacement ACF (τ = 31 mins)
Parallel Fiber Avg. Displacement ACF (τ = 21 mins)
Displacement Autocorrelation Function
1
0.8
0.6
0.4
0.2
0
-0.2
0
50
100
150
200
250
300
Time (mins)

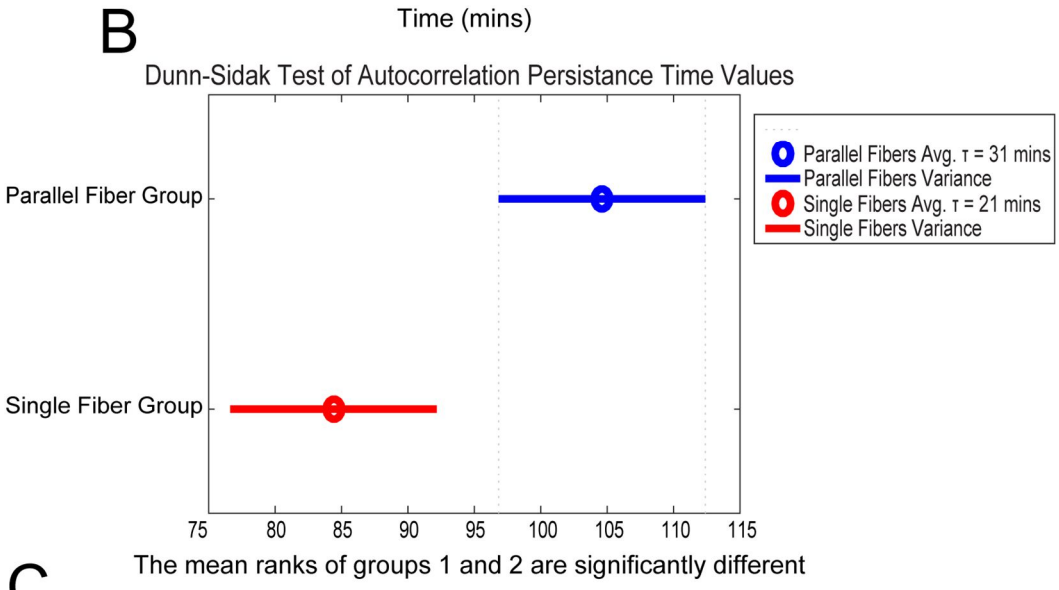
B
Dunn-Sidak Test of Autocorrelation Persistance Time Values
Parallel Fiber Group
Single Fiber Group
Parallel Fibers Avg. τ = 31 mins
Parallel Fibers Variance
Single Fibers Avg. τ = 21 mins
Single Fibers Variance
75
80
85
90
95
100
105
110
115
The mean ranks of groups 1 and 2 are significantly different

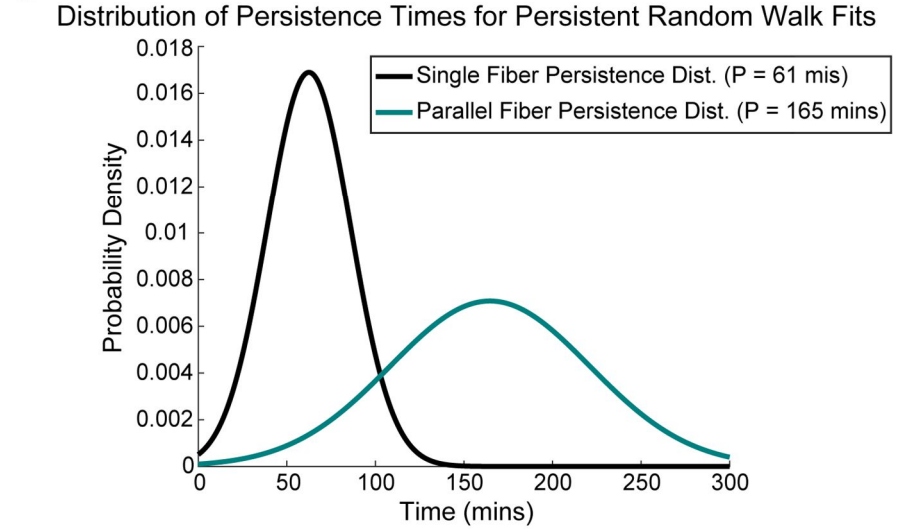
C
Distribution of Persistence Times for Persistent Random Walk Fits
Single Fiber Persistence Dist. (P = 61 mis)
Parallel Fiber Persistence Dist. (P = 165 mins)
Probability Density
0.018
0.016
0.014
0.012
0.01
0.008
0.006
0.004
0.002
0
0
50
100
150
200
250
300
Time (mins)

FIGURE 5

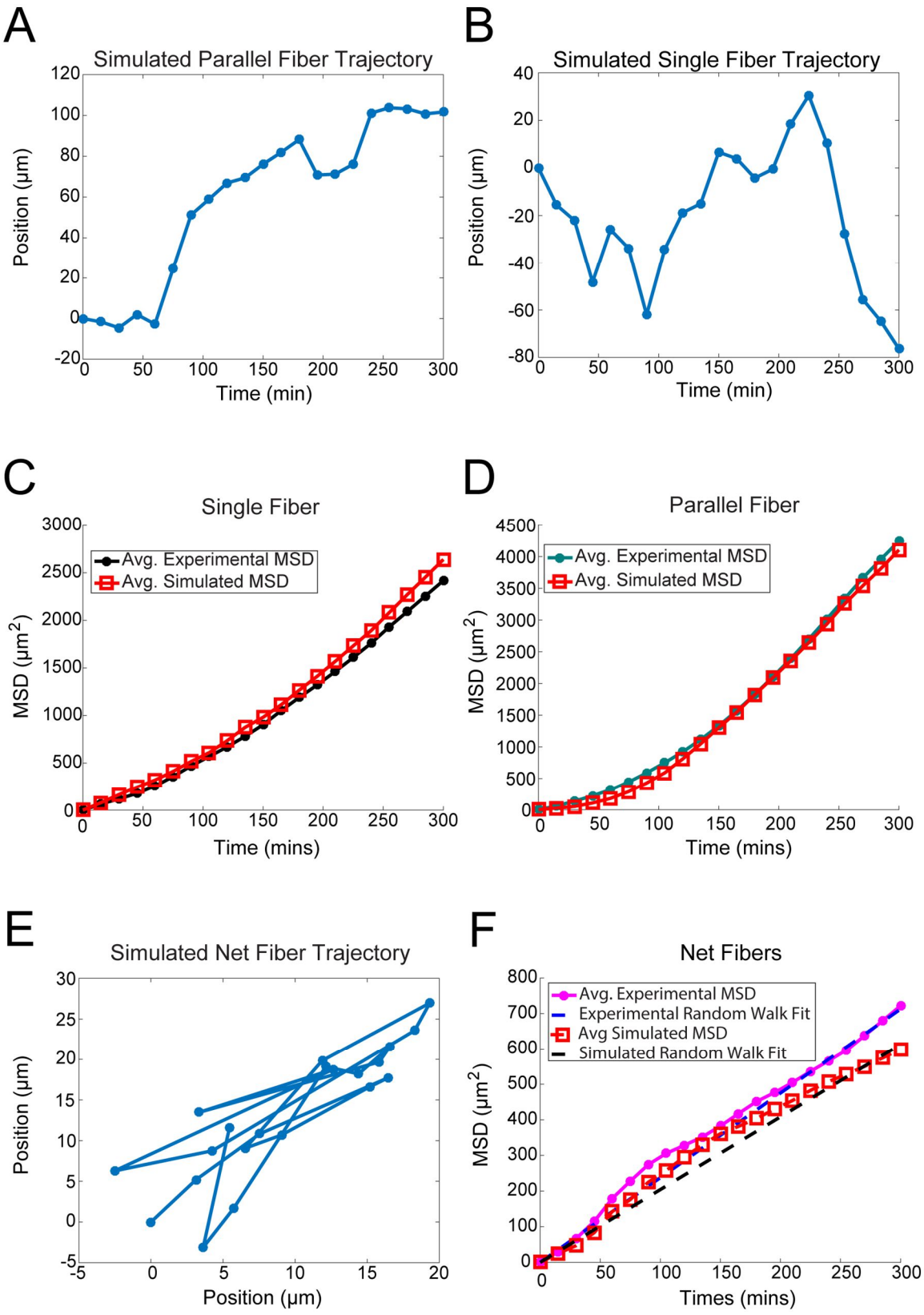
A
Simulated Parallel Fiber Trajectory
Position (μm)
Time (min)
B
Simulated Single Fiber Trajectory
Position (μm)
Time (min)
C
Single Fiber
Avg. Experimental MSD
Avg. Simulated MSD
MSD (μm2)
Time (mins)
D
Parallel Fiber
Avg. Experimental MSD
Avg. Simulated MSD
MSD (μm2)
Time (mins)
E
Simulated Net Fiber Trajectory
Position (μm)
Position (μm)
F
Net Fibers
Avg. Experimental MSD
Experimental Random Walk Fit
Avg Simulated MSD
Simulated Random Walk Fit
MSD (μm2)
Times (mins)

BIBLIOGRAPHY

Baker, Gregory J., Viveka Nand Yadav, Sebastien Motsch, Carl Koschmann, Anda Alexandra Calinescu, Yohei Mineharu, Sandra Ines Camelo-Piragua, et al. 2014. "Mechanisms of Glioma Formation: Iterative Perivascular Glioma Growth and Invasion Leads to Tumor Progression, VEGF-Independent Vascularization, and Resistance to Antiangiogenic Therapy." *Neoplasia (United States)* 16 (7). Neoplasia Press, Inc.: 543–61. doi:10.1016/j.neo.2014.06.003.

Bangasser, Benjamin L., Steven S. Rosenfeld, and David J. Odde. 2013. "Determinants of Maximal Force Transmission in a Motor-Clutch Model of Cell Traction in a Compliant Microenvironment." *Biophysical Journal*. doi:10.1016/j.bpj.2013.06.027.

Cha, Junghwa, Seok-Gu Kang, and Pilnam Kim. 2016. "Strategies of Mesenchymal Invasion of Patient-Derived Brain Tumors: Microenvironmental Adaptation." *Nature Publishing Group*. doi:10.1038/srep24912.

Chan, Clarence E, and David J Odde. 2008. "Traction Dynamics of Filopodia on Compliant Substrates." *Science (New York, N.Y.)* 322 (5908): 1687–91. doi:10.1126/science.1163595.

Curtis, Adam, and Chris Wilkinson. 1997. "Topographical Control of Cells." *Biomaterials* 18 (24): 1573–83. doi:10.1016/S0142-9612(97)00144-0.

Discher, Dennis E, Paul Janmey, and Yu-Li Wang. 2005. "Tissue Cells Feel and Respond to the Stiffness of Their Substrate." *Science (New York, N.Y.)* 310 (5751): 1139–43. doi:10.1126/science.1116995.

Elosegui-Artola, Alberto, Roger Oria, Yunfeng Chen, Anita Kosmalska, Carlos Pérez-González, Natalia Castro, Cheng Zhu, Xavier Trepat, and Pere Roca-Cusachs. 2016. "Mechanical Regulation of a Molecular Clutch Defines Force Transmission and Transduction in Response to Matrix Rigidity." *Nature Cell Biology* 18 (5): 540–48. doi:10.1038/ncb3336.

Faure-andré, Gabrielle, Pablo Vargas, Maria-Isabel Yuseff, Melina Heuze, Jheimmy Diaz, Danielle Lankar, Veronica Steri, et al. 2008. "Regulation of Dendritic Cell Migration by CD74, the MHC Class II–Associated Invariant Chain." *Science* 322 (5908): 1705–10. doi:10.1126/science.1159894.

Fraley, Stephanie I., Yunfeng Feng, Anjil Giri, Gregory D. Longmore, and Denis Wirtz. 2012. "Dimensional and Temporal Controls of Three-Dimensional Cell Migration by Zyxin and Binding Partners." *Nature Communications* 3. Nature Publishing Group: 719. doi:10.1038/ncomms1711.

He, Qiye, Jeff Johnston, Julia Zeitlinger, Kansas City, and Kansas City. 2015. "HHS Public Access" 33 (4): 395–401. doi:10.1038/nbt.3121.ChIP-nexus.

Ivkovic, Sanja, Christopher Beadle, Sonal Noticewala, Susan C. Massey, Kristin R. Swanson, Laura N. Toro, Anne R. Bresnick, Peter Canoll, and Steven S. Rosenfeld. 2012. "Direct Inhibition of Myosin II Effectively Blocks Glioma Invasion in the Presence of Multiple Motogens." *Molecular Biology of the Cell* 23 (4): 533–42. doi:10.1091/mbc.E11-01-0039.

Javid, Samad, Asghar Rezaei, and Ghodrat Karami. 2014. "A Micromechanical Procedure for Viscoelastic Characterization of the Axons and ECM of the

Brainstem." *Journal of the Mechanical Behavior of Biomedical Materials* 30. Elsevier: 290–99. doi:10.1016/j.jmbbm.2013.11.010.

Jiang, Guoying, Grégory Giannone, David R Critchley, Emiko Fukumoto, and Michael P Sheetz. 2003. "Two-Piconewton Slip Bond between Fibronectin and the Cytoskeleton Depends on Talin." *Nature* 424 (6946): 334–37. doi:10.1038/nature01805.

Klank, Rebbeca et al. 2016. "Biphasic Dependence of Glioma Survival and Cell Migration on CD44 Expression Level." *Cell Reports*.

Lämmermann, Tim, and Michael Sixt. 2009. "Mechanical Modes of 'Amoeboid' Cell Migration." *Current Opinion in Cell Biology* 21 (5): 636–44. doi:10.1016/j.ceb.2009.05.003.

Lele, Tanmay P., Charles K. Thodeti, Jay Pendse, and Donald E. Ingber. 2008. "Investigating Complexity of Protein-Protein Interactions in Focal Adhesions." *Biochemical and Biophysical Research Communications* 369 (3): 929–34. doi:10.1016/j.bbrc.2008.02.137.

Marsick, B. M., J. E. San Miguel-Ruiz, and P. C. Letourneau. 2012. "Activation of Ezrin/Radixin/Moesin Mediates Attractive Growth Cone Guidance through Regulation of Growth Cone Actin and Adhesion Receptors." *Journal of Neuroscience* 32 (1): 282–96. doi:10.1523/JNEUROSCI.4794-11.2012.

Molloy, J E, J E Burns, J Kendrick-Jones, R T Tregear, and D C White. 1995. "Movement and Force Produced by a Single Myosin Head." *Nature*. doi:10.1038/378209a0.

Nain, Amrinder S, and Ji Wang. 2013. "Polymeric Nanofibers: Isodiametric Design Space and Methodology for Depositing Aligned Nanofiber Arrays in Single and Multiple Layers." *Polymer Journal* 45: 695–700. doi:10.1038/pj.2013.1.

Odde, D J, E M Tanaka, S S Hawkins, and H M Buettner. 1996. "Stochastic Dynamics of the Nerve Growth Cone and Its Microtubules during Neurite Outgrowth." *Biotechnology and Bioengineering* 50 (4). Piscataway, New Jersey: Biotechnology and Bioengineering: 452–61. doi:10.1002/(SICI)1097-0290(19960520)50:4<452::AID-BIT13>3.0.CO;2-L.

Provenzano, Paolo P, David R Inman, Kevin W Eliceiri, Steven M Trier, and Patricia J Keely. 2008. "Contact Guidance Mediated Three-Dimensional Cell Migration Is Regulated by Rho/ROCK-Dependent Matrix Reorganization." *Biophys J* 95 (11): 5374–84. doi:10.1529/biophysj.108.133116.

Sharma, Puja, Kevin Sheets, Subbiah Elankumaran, and Amrinder Singh Nain. 2013. "The Mechanistic Influence of Aligned Nanofibers on Cell Shape, Migration and Blebbing Dynamics of Glioma Cells." *Integr. Biol. Integr. Biol* 5: 1036–44.

Sniadecki, Nathan J., Ravi A. Desai, Sami Alom Ruiz, and Christopher S. Chen. 2006. "Nanotechnology for Cell-Substrate Interactions." *Annals of Biomedical Engineering* 34 (1): 59–74. doi:10.1007/s10439-005-9006-3.

Wirtz, Denis. 2009. "Particle-Tracking Microrheology of Living Cells: Principles and Applications." *Annual Review of Biophysics* 38: 301–26. doi:10.1146/annurev.biophys.050708.133724.

Wu, Pei-Hsun, Anjil Giri, Sean X Sun, and Denis Wirtz. 2014. “Three-Dimensional Cell Migration Does Not Follow a Random Walk.” *Proceedings of the National Academy of Sciences of the United States of America* 111 (11): 3949–54. doi:10.1073/pnas.1318967111.

Yang, Ya Li, Lindsay M. Leone, and Laura J. Kaufman. 2009. “Elastic Moduli of Collagen Gels Can Be Predicted from Two-Dimensional Confocal Microscopy.” *Biophysical Journal* 97 (7). Biophysical Society: 2051–60. doi:10.1016/j.bpj.2009.07.035.